Temporal evolution of the optical path difference of a supersonic turbulent boundary layer*

Gao Qiong(高 穹)[a)†], Yi Shi-He(易仕和)[b)], Jiang Zong-Fu(姜宗福)[a)], He Lin(何 霖)[b)], and Xie Wen-Ke(谢文科)[a)]

[a)] College of Photon-electron Science and Engineering, National University of Defense Technology, Changsha 410073, China
[b)] College of Aerospace and Material Engineering, National University of Defense Technology, Changsha 410073, China

(Received 13 June 2012; revised manuscript received 4 September 2012)

The density distribution of a supersonic turbulent boundary layer is measured with the nanoparticle-based planar laser scattering technique, and the temporal evolution of its optical path difference (OPD) in a short time interval is characterized by proper orthogonal decomposition (POD). Based on the advantage of POD in capturing the energy of a signal, a temporal evolution model is suggested for the POD coefficients of the OPD. In this model, the first few coefficients vary linearly with time, and the others are modeled by Gaussian statistics. As an application, this method is used to compute the short-exposure optical transfer function.

Keywords: aero-optics, supersonic turbulent boundary layer, optical transfer function

PACS: 42.25.Dd, 47.40.Ki **DOI:** 10.1088/1674-1056/22/1/014202

1. Introduction

Aero-optical aberration because of the compressibility of a high speed flow field serves as a great concern for airborne optical systems, and has attracted much attention for many decades.[1–3] The boundary layer is one of the most important types of flows in aero-optics, and the optical property of a supersonic turbulent boundary layer is the subject of the present paper.

A significant early work on the aero-optics of a boundary layer was by Stine and Winovich.[4] They performed the photometric measurements of a time-averaged radiation passed through a turbulent boundary layer with a Mach number ranging from 0.4 to 2.5. Their work combined together was all that had been known until then on the optical propagation through index-variant turbulent flows. Specifically, the dependence of scattering on the integral scale of the boundary layer was emphasized. Recently, a group from Notre Dame University has paid much attention to the aero-optics of a turbulent boundary layer.[2,5–7] Their experimental measurement was mainly based on the Malley probe and a small-aperture beam technique,[8,9] with which several forms of scaling laws for optical aberration were suggested. Wyckham *et al.*[10] used the Shack–Hartmann wavefront sensor to study the aero-optical distortion of transonic and hypersonic turbulent boundary layers with and without gas injection. A scaling law for the root-mean-square of phase distortion was also proposed, which seems to collapse the data better than previous models. Truman and Lee[11] carried out the direct numerical simulation of an incompressible boundary layer, and regarded the refractive-index as a passive scalar. The effects of organized turbulence structures on the phase aberration were analyzed, and substantial variation with the direction of propagation was found. Tromeur *et al.*[12] and Wand *et al.*[13] did large eddy simulations of aero-optical effects in turbulent boundary layers with transonic and supersonic free streams, and the validity of the linking equation was discussed.

The nano-particle-based planar laser scattering technique (NPLS)[14] recently developed by our group has been used in the study of the aero-optics of supersonic flow.[15–18] The purpose of this paper is to take full advantage of the high spatiotemporal resolution of the NPLS, and to examine the temporal evolution of optical path difference (OPD) of a supersonic turbulent boundary layer in a short time interval. The basic idea here is to construct an optimal basis such that the OPD can be approximated well with just a few terms. For practitioners in optics, the Zernike polynomial is a natural choice to decompose the distorted wavefront, but it is far from being an optimal basis, i.e., a large number of polynomials are required to achieve an accepted approximation. Wavelet and wavelet packet are powerful tools for approximating a signal with quite a small number of transform coefficients,[19] but the basis vectors relevant to the used coefficients are often not fixed, which is rather disadvantageous for further analysis.[18] This paper uses the proper orthogonal decomposition (POD),[20,21] which can offer an optimal basis for the decomposition of the OPD.

2. Experimental apparatus and results

Our experimental apparatus consists of a supersonic boundary layer wind tunnel and an NPLS system, a sketch

*Project supported by the Innovation Research Foundations for Postgraduates of National University of Defense Technology and Hunan Province, China and the National Natural Science Foundation of China (Grant No. 61008037).

†Corresponding author. E-mail: gaoqiong1980@126.com

© 2013 Chinese Physical Society and IOP Publishing Ltd

of the whole setup is shown in Fig. 1. In our experiment, the Mach number of the free stream is 3.0, and the test section dimensions are 120 mm×100 mm. The four walls of the test section are made up of optical glass, and the measurements are made on the boundary layer developed on the wall. More parameters about the experiment can be found in Table 1.

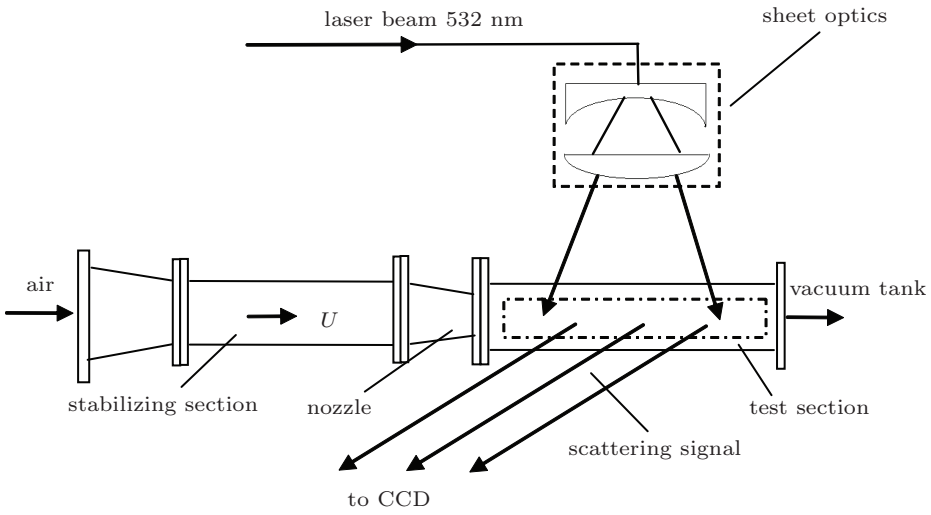


Fig. 1. Sketch of the whole experimental setup including a supersonic wind tunnel and an NPLS system.

Table 1. Important experimental parameters.

M_∞	ρ_∞/kg·m^{-3}	T_0/K	P_0/kPa	Re/m^{-1}	U_∞/m·s^{-1}
3	0.089	300	101.0	7.49×106	620

The NPLS system is composed of a tracer generation system, a light source system, a recording system, and a synchronization system. TiO_2 particles with literal size 18 nm are selected as the tracers. The light source is a dual-cavity Nd:Yag laser (wavelength 532 nm, pulse width 6 ns, energy per pulse 400 mJ). A very thin laser sheet (about 0.5 mm) is generated by the sheet optics system, which illuminates the flow region of interest. The recording system is an interline transfer CCD, and the shortest time interval of double-exposure can reach 0.2 μs by using the inter-frame technique. When the scattering angle is 90° and the polarization direction is perpendicular to the scattering plane, flow images with high signal noise ratios can be captured by the CCD. The synchronizer can adjust the laser emitting and CCD exposure to make sure that the two laser pulses are exactly captured by the double exposures respectively. More details about the NPLS can be found in Ref. [14]. Another recent work of the authors examined the experimental error, which is about 10%.[15]

Figure 2 shows a pair of NPLS images of a supersonic turbulent boundary layer in the side view plane. The flow is from the left to the right. The physical size of the images is 27 mm×11.7 mm, the digital resolution of a pixel is about $h = 0.017$ mm, and the time interval between the two images is 5 μs. A rough estimation of the viscous length gives a value in the order of 1 μm, and the thickness of the boundary layer is about $\delta = 10.2$ mm. The bottom of the image is adjacent to the plate. Because of the influence of diffuse reflection, the flow structure just above the plate (approximately with the height of $50h$) is almost invisible. The image above this zone shows the density structure of the supersonic turbulent boundary layer, and the coherent structures can be seen easily. In particular, the time evolution of the flow structure in the short time interval can be checked.

Tian *et al.*[22] demonstrated the linear relationship between the intensity of an NPLS image and the density, and developed a calibration procedure by using the jump of density before and behind a shock wave. Here that method is employed to convert the image intensity into a density distribution. With the density, the optical path length (OPL) is computed as

$$\mathrm{OPL}(x) = \int_{y_a}^{y_b} n(x,y)\,\mathrm{d}y = \int_{y_a}^{y_b} [1 + K_{GD}\rho(x,y)]\,\mathrm{d}y, \quad (1)$$

where y_a and y_b are the lower and the upper boundaries of the flow region in the vertical direction, respectively, and K_{GD} is the Gladstone–Dale constant. In this study, we choose $K_{GD} = 2.2 \times 10^{-4}$ m^3/kg, and the relevant wavelength is $\lambda = 0.5$ μm. The OPD is defined as

$$\mathrm{OPD}(x) = \mathrm{OPL}(x) - \langle \mathrm{OPL}(x) \rangle, \quad (2)$$

where the bracket denotes the average over the aperture. In Fig. 3, we show the OPD relevant to the flow in Fig. 2. The basic profile of the OPD is due to the large scale structure of the layer, and the small amplitude jumps can be attributed to the fine structure of the flow and the experimental error.

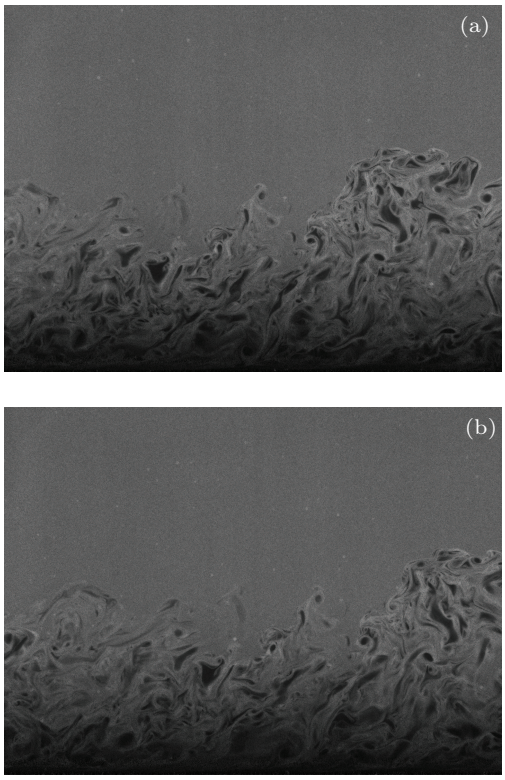


Fig. 2. A pair of temporal correlated NPLS images of the supersonic turbulent boundary layer with free stream Mach number 3.0. The flow is from the left to the right, and the time interval of the two images is 5 μs, i.e., (a) $t = t_0$ μs and (b) $t = t_0 + 5$ μs. The two images have been enhanced by power-law transform with $\gamma = 0.6$. The images used in our calculation below are the original ones.

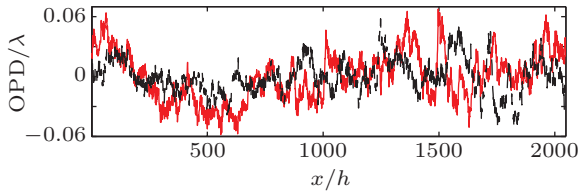


Fig. 3. (color online) The OPD relevant to the images in Fig. 2 (red solid line: Fig. 2(a), black dashed line: Fig. 2(b)).

3. Temporal evolution model

Our work about the evolution of the OPD in a short time interval relies heavily on the proper orthogonal decomposition (POD), which has been used extensively in constructing low order models for turbulence.[20,21] The basis vectors of the POD are constructed with an ensemble of relevant signals, and any signal in the ensemble can be approximated well with a linear combination of just a few basis vectors.

Suppose that we have a set of realizations of the OPD of the supersonic mixing layer $\{L_i | i=1, 2, \ldots, M\}$, each L_i has the size of $N \times 1$, and the POD basis $\{\psi_j\}$ and eigenvalues $\{\lambda_j\}$ are also obtained. We study a pair of OPD $\{L(t_1), L(t_2)\}$ in the ensemble, and the time interval t_2–t_1 is not larger than the convective time t_c of the large scale structure. Based on the results of Smith *et al.*[23] and Poggie *et al.*,[24] the convection velocity of the large scale structure in the supersonic boundary layer is approximately $0.9U_\infty$, so the convective time is $t_c = \delta/0.9U_\infty \approx 18$ μs. With the POD basis, the pair of the OPD can be expressed as

$$L(t_1) = \sum_j a_j(t_1)\psi_j, \quad L(t_2) = \sum_j a_j(t_2)\psi_j. \tag{3}$$

We can find from Eq. (3) that if we can obtain the coefficients a_j in a short time interval, the time evolution of OPL is obtained equivalently. Based on the extensive applications of POD in the study of turbulence,[20,21] we know that the POD bases of the first few orders correspond to the large scale structures, and slow variations of the relevant coefficients are expected. The bases of high orders correspond to the subtle structure, so the evolutions of high order POD coefficients may be random even in a short time interval. Based on this, two hypothesizes are assumed.

H1 There exists an integer P much smaller than N such that the first P POD coefficients vary linearly with time in a short time interval.

H2 The POD coefficients of larger orders can be modeled by Gaussian statistics $a_j \sim N(0, \lambda_j)$, $j > P$.

The two hypothesizes constitute a mixed model for the temporal evolution of POD coefficients, in which both deterministic and random factors are included. The Gaussian assumption in H2 is often used in turbulence research. Another useful property of the POD coefficients is

$$\langle a_j a_k \rangle = \delta_{jk}\lambda_j. \tag{4}$$

These two points will be checked in the following. We note that the choice of P is not so explicit and depends on a certain problem and specific requirements. We will discuss this problem when applying the theory in the next section.

In this work, a snapshot method is used to compute the POD eigenvectors and eigenvalues, and the details of implementation can be found in Ref. [21]. With an ensemble of 200 OPDs of the boundary layer, the POD eigenvectors and eigenvalues are shown in Fig. 4. The eigenvalues are shown in Fig. 4(a) with red dots, from which we can see that the eigenvalue decays dramatically with the increasing order. This fact validates the efficiency of the POD for capturing the energy of a signal. The eigenvectors of the second and fourth orders are shown in Fig. 4(b). As the order increases, the oscillation trend of the eigenvector becomes evident. This phenomenon is similar to that in a Fourier analysis to some extent. The variance of a_k is displayed in Fig. 4(a) with black crosses, which agrees with the eigenvalue λ_k very well. In addition, the mean of a_k is very close to zero, so the assumption $a_k \sim N(0, \lambda_k)$ is validated.

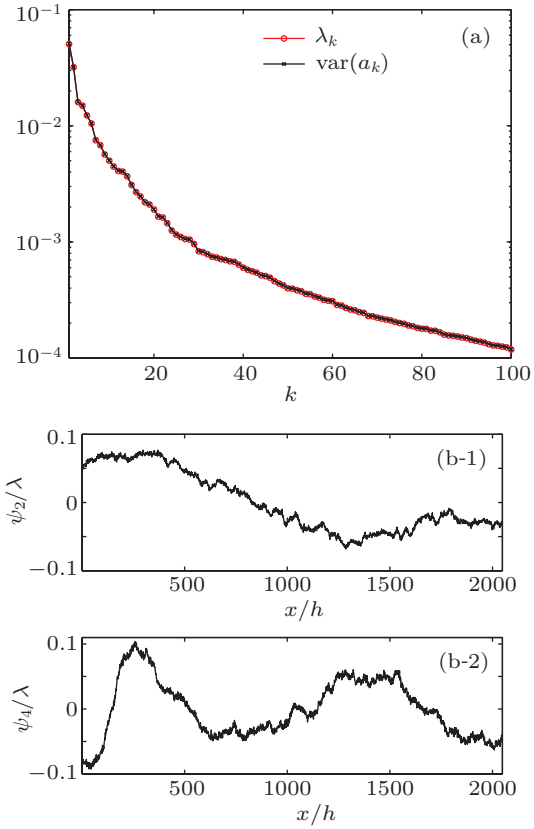


Fig. 4. (color online) POD analysis of OPD: (a) POD eigenvalues (red dot) and the variance of a_k (black cross), and POD eigenvectors of (b-1) the second and (b-2) the fourth orders.

4. Computation of short-exposure OTF

We know that the optical transfer function (OTF) is the most important measurement of an optical imaging system.[25,26] Following on from the measurement of the OPD in Section 2 and the model in Section 3, we will compute the short-exposure OTF of a supersonic boundary layer. Let us denote

$$W(t,x) = 2\pi L(t,x)/\bar{\lambda}, \tag{5}$$

where $\bar{\lambda}$ is the averaged wavelength of the imaging system, and is 0.5 μm in our computation. For the one-dimensional (1D) case here, the instantaneous incoherent OTF can be written as[26]

$$H(t,f_x) = \int_{l(f_x)} \exp\{\mathrm{i}[W(t,x+\bar{\lambda}df_x/2) - W(t,x-\bar{\lambda}df_x/2)]\}\mathrm{d}x \Big/ \int_{l(0)} \mathrm{d}x, \tag{6}$$

where d is the imaging distance, and $l(f_x)$ is the overlapping area of two shifted apertures

$$p(x+\bar{\lambda}df_x), \quad p(x-\bar{\lambda}df_x). \tag{7}$$

For an aperture of rectangular shape used in our computation,

$$p(x) = \mathrm{rect}\left(\frac{x}{2w}\right) = \begin{cases} 1, & |x| < w, \\ 0, & \text{else}, \end{cases} \tag{8}$$

where w is the half width of the aperture. We also define a truncating frequency f_0 and a normalized frequency as

$$f_0 = w/\bar{\lambda}d, \quad \hat{f}_x = f_x/2f_0. \tag{9}$$

It is simple to validate that the OTF of an ideal rectangular aperture of half width w is

$$H(\hat{f}_x) = 1 - \hat{f}_x, \quad \hat{f}_x \le 1. \tag{10}$$

Before the computation, we note that the overall amplitude of the OPD in Fig. 3 is about 0.1λ, so the influence of the distortion on imaging is expected to be slight. In fact, we have computed the short-exposure OTF with the original OPD, and find out that its deviation from the ideal OTF is small. It seems that the aero-optical aberration of the supersonic boundary layer can be neglected. However, in practice, this is not such a problem. The above data are obtained directly with the wind tunnel experiments on the ground. If we apply the result to the estimation of aero-optical effects in practice, a proper transformation is necessary. The scaling law of $\mathrm{OPD}_{\mathrm{rms}}$ has been examined by many researchers.[5,7,10] Wyckham *et al.*[10] investigated this problem for tran- and hyper-sonic turbulent boundary layers, their result indicated that the $\mathrm{OPD}_{\mathrm{rms}}$ is proportional to the free stream density. For vehicles with an altitude of 10 km, the density of the atmosphere is 0.414 kg·m^{-3}, and is about 4.6 times the value in our experiment. We use the original OPD multiplied by 5 in the computation given below.

As mentioned in the previous subsection, determining a proper number of POD coefficients with deterministic temporal evolution is an important problem. Here we deal with this problem from the viewpoint of cumulative energy. With a set of eigenvalues of POD $\{\lambda_i\}$, the cumulative energy is defined as

$$e(k) = \sum_{i=1}^{k} \lambda_i / \sum_i \lambda_i. \tag{11}$$

For the ensemble of the OPD used here, the cumulative energy curve is shown in Fig. 5(a). It can be found that the cumulative energy increases quickly with k and approaches 1. Here we choose three points on the curve, $e(11) = 70.9\%$, $e(18) = 80.4\%$, and $e(39) = 90.3\%$. Setting P as 11, 18, and 39, we compute the OTF with exposure time 10 μs, the relevant amplitudes are shown in Fig. 5(b). We can see that the OTF with a larger P has a smaller amplitude, but the difference is not evident. This phenomenon has been validated by more computations. It seems that choosing such a number of P that $e(P)$ is about 80% is ideal. In fact, too many deterministic coefficients will cancel the randomness in the evolution of OPD, which is not expected. Another problem in the computation short-exposure OTF is how many realizations of OPD are enough to obtain a convergent average. Our computation experience shows that 50 realizations of OPD are sufficient for an exposure time not larger than 20 μs.

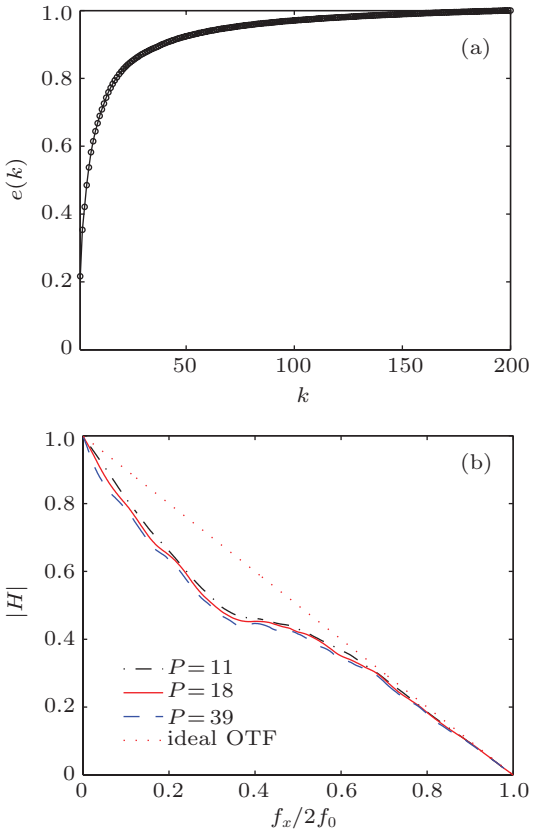


Fig. 5. (color online) (a) Cumulative energy of the POD analysis. (b) Amplitudes of OTF with exposure time 10 μs for different P.

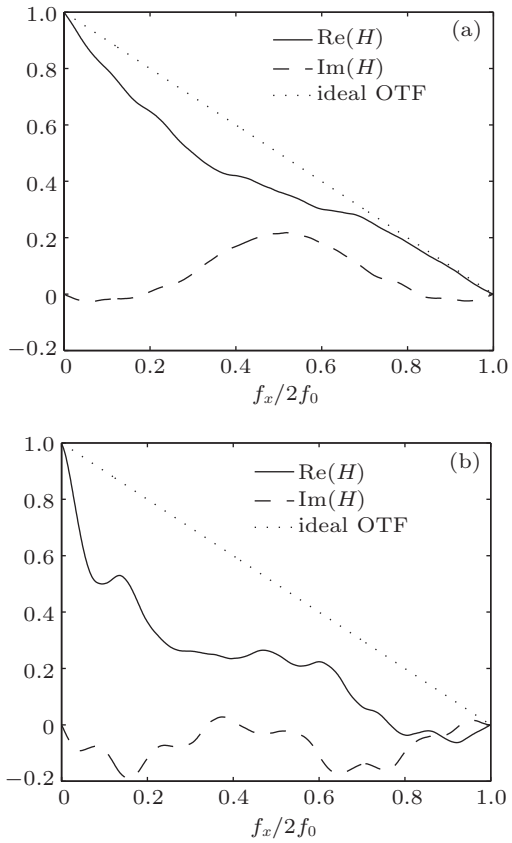


Fig. 6. OTF of the supersonic boundary layer with exposure time (a) 10 μs and (b) 20 μs.

Figure 6 shows the real and imaginary parts of the OTF with exposure time 10 μs and 20 μs, and the results in Fig. 6(a) are relevant to the OTF in Fig. 5(b) with $P = 18$. Obviously, the influence of aero-optical distortion on imaging is evident, especially for low spatial frequencies. However, the deviation from the ideal OTF at a high frequency is not noticeable. This point may be investigated further in the reconstruction of objects, which is similar to the application of speckle interferometry in astronomical imaging.[27] Another feature of the OTF is its imaginary part with a considerable amplitude. Here it is worth comparing our result with the early work of Steinmetz.[28] The Gaussian assumption of OPD was used frequently in the early study of aero-optics.[1] With this assumption, Steinmetz asserted that the OTF should be real values. But the discovery of coherent structures in a shear layer challenges this assumption. Our recent work examined this problem by extracting the coherent structures of the OPD of a supersonic mixing layer, and provided quantitative arguments against the assumption.[18] Here we directly compute the skewness and the flatness of the OPD used in the computation of OTF in Fig. 6, and the results are (0.45, 3.02) and (1.05, 5.33), respectively. Hence the Gaussian assumption cannot be justified reasonably.

5. Conclusion

We have measured the density distribution of a supersonic turbulent boundary layer with the NPLS technique, and the time evolution of its OPD is characterized by a POD analysis. In order to obtain the OPD at any time instant in the time intervals, the OPD is decomposed with POD eigenvectors, and a model for the time evolution of the POD coefficients is suggested to achieve this purpose. In this model, the first few POD coefficients are assumed to vary linearly with time, and the others are modeled with Gaussian statistics, so the deterministic and the random factors are combined together. As an application of our theory, the short-exposure OTF of a supersonic turbulent layer is computed and analyzed.

References

[1] Gilbert K G and Otten L J 1982 *Aero-Optical Phenomena* (New York: AIAA)
[2] Jumper E J and Fitzgerald E J 2001 *Prog. Aerospace. Sci.* **37** 299
[3] Wang W, Mani A and Gordeyev S 2012 *Ann. Rev. Fluid. Mech.* **44** 299
[4] Stine H A and Winovitch W 1956 *NACA Res. Mem.* A56B21
[5] Gordeyev S, Jumper E J, Ng T T and Cain A B 2003 *AIAA paper* 2003-3606
[6] Gordeyev S, Cress J A and Jumper E J, *Aero-Optical Properties of Subsonic, Turbulent Boundary Layers* (preprint)
[7] Gordeyev S, Jumper E J and Hayden T E 2011 *AIAA paper* 2011-1325
[8] Malley M, Sutton G W and Kincheloe N 1992 *Appl. Opt.* **31** 4440
[9] Hugo R J and Jumper E J 1996 *Appl. Opt.* **35** 4436
[10] Wyckham C M and Smith A J 2006 *AIAA paper* 2006-3067

[11] Truman C R and Lee M J 1992 *AIAA paper* 1992-2817
[12] Tromeur E, Garnier E and Sagaut P 2006 *J. Turbulence* **7** 1
[13] Wang K and Wang W 2011 *AIAA paper* 2011-3278
[14] Zhao Y X, Yi S H, Tian L F and Cheng Z Y 2009 *Sci. China Ser.* E **52** 3640
[15] Gao Q, Yi S H, Jiang Z F, He L and Zhao Y X 2012 *Opt. Express* **20** 16494
[16] Yi S H, Tian L F, Zhao Y X, He H and Cheng Z Y 2010 *Chin. Sci. Bull.* **55** 3545
[17] Gao Q, Jiang Z F, Yi S H and Zhao Y X 2010 *Appl. Opt.* **49** 3786
[18] Gao G, Yi S H, Jiang Z F, Zhao Y X and Xie W K 2012 *Chin. Phys.* B **21** 064701
[19] Mallat S A 2003 *Wavelet Tour of Signal Processing* (Singapore: Elsevier)
[20] Berkooz G, Holmes P and Lumley J L 1993 *Ann. Rev. Fluid Mech.* **25** 539
[21] Holmes P, Lumley J L and Berkooz G 1996 *Turbulence, Coherent Structures, Dynamical Systems and Symmetry* (Cambridge: Cambridge University Press)
[22] Tian L F, Yi S H, Zhao Y X, He L and Cheng Z Y 2009 *Sci. China Ser.* G **52** 1357
[23] Smits A J, Spina E F, Alving A E, Smith R W, Fernando E M and Donovan J F 1989 *Phys. Fluids* A **1** 1865
[24] Poggie J, Erbland P J, Smits A J and Miles R B 2004 *Exp. Fluids* **37** 438
[25] Williams C W and Becklund O A 1989 *Introduction to the Optical Transfer Function* (New York: John Wiley & Sons)
[26] Goodman J W 1996 *Introduction to Fourier Optics* (New York: McGraw-Hill)
[27] Goodman J W 2007 *Speckle Phenomena in Optics*: *Theory and Applications* (Englewood: Ben Roberts & Company)
[28] Steinmetz W J 1982 *Aero-Optical Phenomena* (New York: AIAA) pp. 78–100